

Detection of Atypical H-Type Bovine Spongiform Encephalopathy and Discrimination of Bovine Prion Strains by Real-Time Quaking-Induced Conversion

Kentaro Masujin,^{a,b} Christina D. Orrú,^a Kohtaro Miyazawa,^b Bradley R. Groveman,^a Lynne D. Raymond,^a Andrew G. Hughson,^a Byron Caughey^a

Laboratory of Persistent Viral Diseases, Rocky Mountain Laboratories, National Institute of Allergy and Infectious Diseases, National Institutes of Health, Hamilton, Montana, USA^a; Influenza and Prion Disease Research Center, National Institute of Animal Health, National Agriculture and Food Research Organization, Tsukuba, Japan^b

Prion diseases of cattle include the classical bovine spongiform encephalopathy (C-BSE) and the atypical H-type BSE (H-BSE) and L-type BSE (L-BSE) strains. Although the C- and L-BSE strains can be detected and discriminated by ultrasensitive real-time quaking-induced conversion (RT-QuIC) assays, no such test has yet been described for the detection of H-BSE or the discrimination of each of the major bovine prion strains. Here, we demonstrate an RT-QuIC assay for H-BSE that can detect as little as 10⁻⁹ dilutions of brain tissue and neat cerebrospinal fluid samples from clinically affected cattle. Moreover, comparisons of the reactivities with different recombinant prion protein substrates and/or immunoblot band profiles of proteinase K-treated RT-QuIC reaction products indicated that H-, L-, and C-BSE have distinctive prion seeding activities and can be discriminated by RT-QuIC on this basis.

Many mammalian species can be afflicted with prion diseases or transmissible spongiform encephalopathies. Prion diseases are neurodegenerative, transmissible, untreatable, and fatal (reviewed in references 1 and 2). The underlying pathogenesis of prion diseases involves the conversion of the host's normal prion protein, PrP^C, to abnormal forms that are usually more protease resistant, multimeric, and insoluble. The multimeric and insoluble forms have been generically called PrP^{Sc} (PrP-*scrapie*), or more functionally PrP^{Res} (protease resistant) and PrP^D (disease associated). At least some of these forms comprise the transmissible agent or prion (3–10). Multiple prion strains can be propagated within a given host species, giving consistently different clinical, pathological, and molecular phenotypes (11–16).

The first prion disease to be recognized in cattle was classical bovine spongiform encephalopathy (C-BSE). C-BSE was likely caused primarily by widespread prion contamination of cattle feed (17). After peaking in the early 1990s, the incidence of C-BSE has now been greatly reduced by regulatory measures that limit its horizontal spread. C-BSE is the only known zoonotic prion disease, having caused variant Creutzfeldt-Jakob disease (vCJD) in humans who presumably consumed contaminated beef. Although new clinical cases of vCJD are rare (<http://www.cjd.ed.ac.uk/documents/figs.pdf>), a recent survey of appendices in the United Kingdom suggests a high incidence of subclinical vCJD infections, at ~1:2,000 of the population born between 1941 and 1985 (18).

Since the C-BSE epidemic, two atypical strains of BSE, H-type BSE (H-BSE) and L-type BSE (L-BSE), have also been identified in cattle. PrP^{Res} is usually composed of a mixture of glycosylated and unglycosylated molecules, and the various BSE strains can be differentiated biochemically using Western blotting of postmortem brain tissue samples by comparing the proteinase K (PK)-treated PrP^{Res} banding patterns (19–22). The H and L types of BSE are classified by their respective high and low apparent molecular masses of the unglycosylated PrP^{Res} band. These atypical BSE strains, which are rare (<100 cases identified worldwide), tend to

affect older animals (23) and appear to represent sporadic forms of bovine prion diseases (24). Despite the apparent rarity of the various types of BSE, the facts that H- and L-BSE appear to arise spontaneously and have distinct transmissibilities (20, 25–32) make it important to be able to detect and differentiate them to reduce the risk of transmission to cattle or other species, such as humans.

Several *in vitro* methods have been developed to detect C-, L-, and H-BSE. Commercially available rapid immunochemical tests for PrP^D can, in the best cases, give positive responses from 10⁻³ to 10⁻⁴ dilutions of postmortem brain tissues with high levels of PrP^D (33, 34). Immunoblotting for PrP^{Res} can detect BSE-infected tissues with similar sensitivity and also discriminate between the bovine strains based on the relative electrophoretic migration and glycoform ratios of the PrP^{Res} bands (19–22). A more sensitive conformation-dependent immunoassay (CDI) has also been described for C-BSE, which has a sensitivity similar to that of endpoint dilution bioassays in a line of transgenic mice expressing bovine PrP [Tg(BoPrP^{+/+})4092-*Prnp*^{0/0}], that is, with 50% positive responses at C-BSE brain dilutions of ~10⁻⁵ (35). Another line of “bovinized” transgenic mice has been reported to be 5- to 10-fold-more sensitive in detecting dilutions of BSE brain tissue (36). Still more-sensitive protein-misfolding cyclic amplification

Received 9 October 2015 Returned for modification 6 November 2015

Accepted 25 December 2015

Accepted manuscript posted online 6 January 2016

Citation Masujin K, Orrú CD, Miyazawa K, Groveman BR, Raymond LD, Hughson AG, Caughey B. 2016. Detection of atypical H-type bovine spongiform encephalopathy and discrimination of bovine prion strains by real-time quaking-induced conversion. *J Clin Microbiol* 54:676–686. doi:10.1128/JCM.02731-15.

Editor: B. W. Fenwick

Address correspondence to Byron Caughey, bcaughey@nih.gov.

K. Masujin and C. D. Orrú contributed equally to this study.

Copyright © 2016, American Society for Microbiology. All Rights Reserved.

(PMCA) assays have also been developed for C-BSE in cattle, which can detect brain tissue dilutions down to 10^{-10} (37–39). However, these PMCA assays require 4 to 8 days for this level of sensitivity and are more technically demanding than is optimal for routine diagnostic purposes.

Previous efforts to improve the practicality and performance of testing for bovine prions led to the adaptation of a highly sensitive and specific assay called *real-time quaking-induced conversion* (RT-QuIC) for the detection and discrimination of C-BSE and L-BSE (40). RT-QuIC is based upon the prion-seeded assembly of protease-sensitive recombinant PrP^C (rPrP^{Sen}) into thioflavin T (ThT)-positive amyloid fibrils (41, 42). The reactions are performed in multiwell plates that are intermittently shaken in a fluorescence plate reader, providing a relatively high-throughput and feasible system for prion disease diagnosis. Here, we describe ultrasensitive RT-QuIC assays for detecting H-BSE and for discriminating all three of the bovine BSE strains.

MATERIALS AND METHODS

Ethics statement. The brain tissue and cerebrospinal fluid (CSF) samples from cattle experimentally inoculated intracerebrally with either the C-, L-, or H-BSE prion strain were obtained from the National Institute of Animal Health (NIAH), National Agriculture and Food Research Organization (NARO), Japan (25, 43, 44). These samples were collected at the terminal stage of disease (C-BSE, 22.5 months postinoculation; L-BSE, 16.2 months postinoculation; and H-BSE, 18.7 months postinoculation), in accordance with the regulations outlined in *Guide for the Care and Use of Laboratory Animals* of the NIAH (62) and *Guidelines for Proper Conduct of Animal Experiments* of the Science Council of Japan (63). Procedures involving animals were approved by the Institutional Animal Care and Use Committee at the NIAH (approval numbers 10-005, 11-008, and 13-005).

Western blot analysis of PrP^{Res} from C-, L-, or H-BSE-affected cattle. Brain tissue (cortex) samples from uninfected, C-, L-, or H-BSE-affected cattle were homogenized (20% concentration [wt/vol]) in phosphate-buffered saline (PBS) using a multibead shaker (Yasui Kikai). The brain homogenates (125 μ l) were mixed with an equal volume of buffer containing 4% (wt/vol) Zwittergent 3-14 (Calbiochem), 1% (wt/vol) Sarkosyl, 100 mM NaCl, and 50 mM Tris-HCl (pH 7.6) and incubated with 1 mg/ml collagenase at 37°C for 1 h. Next, the samples were subjected to PK (Roche Diagnostics) digestion (40 μ g/ml) at 37°C for 1 h. PK digestion was terminated with Pefabloc (Roche Diagnostics). The samples were mixed with an equal volume of a 2-butanol-methanol mixture (5:1) and centrifuged at 20,000 \times g for 10 min. The pellets were resuspended in gel-loading buffer containing 2% (wt/vol) SDS and boiled for 10 min prior to loading the gel. The samples were separated by SDS-PAGE (12% acrylamide) and transferred onto a polyvinylidene difluoride (PVDF) membrane (Millipore). The membrane was then incubated with horseradish peroxidase (HRP)-conjugated monoclonal antibody (MAb) T2 at a 1:5,000 dilution (45). Fluorescence signals were detected by incubating the membrane with a chemiluminescent reagent (SuperSignal; Pierce Biotechnology).

Recombinant prion protein expression and purification. rPrP^{Sen} substrates were prepared, as previously described (46). Briefly, the PrP sequence for bank vole (BV) (residues 23 to 230, methionine at residue 109 [M₁₀₉], GenBank accession no. AF367642; residues 23 to 230, isoleucine at 109 [I₁₀₉]; and residues 90 to 230, M₁₀₉), Syrian golden hamster (Ha) (residues 23 to 231, GenBank accession no. K02234; and residues 90 to 231), mouse (residues 23 to 231, GenBank accession no. M13685), sheep (Sh) (residues 25 to 234, ARQ, [alanine at 136 {A₁₃₆}/arginine at 154 {R₁₅₄}/glutamine at 171 {Q₁₇₁}], GenBank accession no. AY907689; VRQ [valine at 136 {V₁₃₆}/R₁₅₄/Q₁₇₁], GenBank accession no. AJ567988.1; ARR [A₁₃₆/R₁₅₄/R₁₇₁]), human (Hu) (residues 23 to 231, methionine at 129 [M₁₂₉]), human-bank vole chimera (Hu-BV) (human residues 23 to 165,

followed by bank vole residues 166 to 230, M₁₀₉), and a hamster-sheep (Ha-S) chimera (Syrian hamster residues 23 to 137, followed by sheep residues 141 to 234 of the R₁₅₄/Q₁₇₁ polymorph, GenBank accession no. AY907689) were amplified and ligated into the pET41 vector (EMD Biosciences), and the sequences were verified. Vectors were transformed into *Escherichia coli* Rosetta(DE3) and were grown in Luria broth medium in the presence of kanamycin and chloramphenicol. Protein expression, purification, and refolding were performed, as previously described (46, 47). The eluted protein was extensively dialyzed into 10 mM sodium phosphate buffer (pH 5.8) and then filtered with a 0.22- μ m syringe filter (Fisher) and stored at -80°C until use. Protein concentration was determined by measuring the absorbance at 280 nm.

Brain homogenate preparation for RT-QuIC. Brain homogenates (BH) (10% [wt/vol]) were prepared, as previously described (41), and stored at -80°C . For RT-QuIC analysis, brain homogenates were serially diluted in 0.1% SDS-N₂ (Gibco)-PBS, as previously reported (48); where indicated, the last dilution was performed in 0.05% SDS-N₂-PBS.

RT-QuIC analysis. RT-QuIC reactions were performed as previously described (41). The RT-QuIC reaction mixture was composed to give final reaction concentrations of 10 mM phosphate buffer (pH 7.4), 300 mM or 130 mM NaCl, 10 μ M thioflavin T (ThT), 1 mM EDTA, 0.1 mg/ml rPrP^{Sen}, and 0.002% or 0.001% SDS. A volume of this mixture (98 μ l for BH or 80 μ l for CSF) was loaded into each well of a black 96-well plate with a clear bottom (Nunc) and seeded with 2 μ l of BH dilution or 20 μ l of CSF. Uninfected bovine BH dilutions or CSF samples were used as negative controls. The plate was sealed with a plate sealer film (Nalge Nunc International) and incubated at either 42°C or 55°C for 40 to 90 h in a BMG FLUOstar Omega plate reader with cycles of 1 min of shaking (700 rpm double orbital) and 1 min of rest throughout the incubation. ThT fluorescence measurements (excitation, 450 \pm 10 nm; emission, 480 \pm 10 nm, bottom read) were taken every 45 min. The RT-QuIC data were analyzed as previously described (49). Briefly, to compensate for differences between the fluorescence plate readers, data sets from replicate wells were averaged and normalized to a percentage of the maximal fluorescence response of the instrument, and the obtained values were plotted against the reaction times. Samples were judged to be RT-QuIC positive using previously described criteria (47). The data are displayed as the averages and standard deviations of the results from four technical replicates, except where indicated.

SD₅₀ calculations. The 50% seeding dose (SD₅₀) was determined by endpoint dilution RT-QuIC, as previously described (41). Briefly, a dilution series with at least one dilution giving 100% ThT-positive replicates and at least one dilution giving 0% ThT-positive replicates was chosen for Spearman-Kärber analysis. SD₅₀ was defined as the amount giving positive ThT fluorescence in 50% of the replicate wells.

PK digestion of RT-QuIC products and Western blot analysis. PK treatment of RT-QuIC BV rPrP^{Sen} conversion products and immunoblotting were performed as previously described (47). RT-QuIC reaction products were collected from the bottom of plates by extensive scraping and pipetting using the same tip for all replicate wells and treated with 10 μ g/ml PK for 1 h at 37°C with orbital shaking at 400 rpm to leave PK-resistant recombinant PrP (rPrP^{Res}) products. The samples were then mixed with an equal volume of gel-loading buffer containing 10% SDS and 8 M urea and were boiled for 10 min for Western blot analysis. The samples were separated using a 12% NuPAGE gel (Novex) and transferred onto a PVDF membrane (Millipore). The blotted membrane was then incubated with R20 primary antiserum (hamster epitope, residues 218 to 231) (50), followed by an anti-rabbit alkaline phosphatase (AP)-conjugated secondary antibody. Signals were visualized using AttoPhos AP fluorescent substrate system (Promega). The rPrP^{Res} band ratio was calculated by using ImageQuant TL software (GE Healthcare).

RESULTS

Immunoblot profile of PrP^{Res} in brain samples from BSE-infected cattle. The brain samples (cortex) were collected from cat-

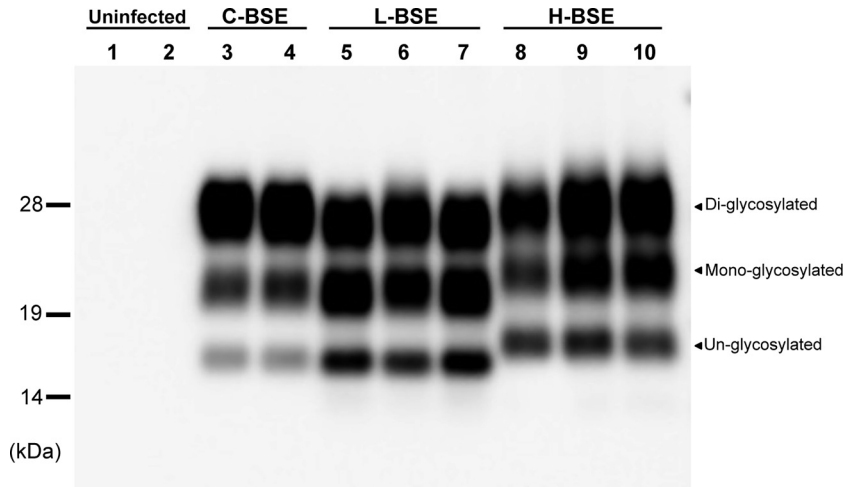


FIG 1 Western blot analysis of PrP^{Res} in brain homogenate samples from cattle affected by C-BSE, L-BSE, or H-BSE. The immunoblot was probed with an HRP-conjugated MAb T2. Lanes 1 and 2, uninfected cattle; lanes 3 and 4, C-BSE ($n = 2$); lanes 5 to 7, L-BSE ($n = 3$); lanes 8 to 10, H-BSE ($n = 3$). All the samples were digested with 40 $\mu\text{g/ml}$ PK at 37°C for 1 h. Molecular markers are shown on the left in kilodaltons.

tle affected by C-, L-, or H-BSE. To confirm the presence of PrP^{Res} in the brain specimens and the presence of the typical banding pattern profiles of C-, L-, and H-BSE, the samples were treated with PK and analyzed by Western blotting. As expected (Fig. 1), and as previously described (19), the H-BSE samples all showed a predominance of the highest-molecular-weight glycoform and unglycosylated (Fig. 1, middle row) and monoglycosylated (Fig. 1, lowest row) bands that migrated slightly above the corresponding bands in the C- and L-BSE profiles.

H-BSE detection using BV rPrP^{Sen}. Given that full-length wild-type BV rPrP^{Sen} with residues 23 to 230 and methionine at residue 109 (BV rPrP^{Sen} 23–230, M₁₀₉) has recently been shown to serve as an apparently universal substrate for RT-QuIC detection of prions of all species and strains tested so far (47), we first tested BV rPrP^{Sen} as a substrate for detecting H-BSE. Reaction mixtures seeded with 10^{-5} dilutions of brain tissue samples from three cattle clinically affected with H-BSE gave rapid increases in ThT fluorescence within 5 h (Fig. 2). In contrast, reaction mixtures seeded with the same dilution of brain samples from C-BSE-infected cattle gave much longer lag phases of between 24 and 40 h, while L-BSE reactions consistently displayed intermediate lag phases of 8 to 13 h. For one C-BSE sample, when reaction mixtures were seeded with 10^{-5} dilutions of brain tissue, RT-QuIC kinetics were only $\sim 20\%$ faster than in an uninfected negative-control brain homogenate, which started to give spontaneous and prion-independent positive fluorescence after 50 h. The 50-h reaction time therefore marked the point at which it became difficult to clearly discriminate prion-seeded reactions from spontaneously positive reactions; this point is known to vary with substrate, reaction conditions, and sample matrix effects (41, 47, 51, 52). These results indicated that with RT-QuIC using the BV rPrP^{Sen} substrate, H-BSE was consistently more rapidly detectable than with either C-BSE or L-BSE at the same concentration of brain homogenate from clinically affected animals.

To assess the analytical sensitivity for detecting H-BSE seeding activity in brain tissue from clinical animals, we performed end-point dilution analysis on samples from the three infected cattle. For each case, all brain tissue dilutions down to 10^{-8} gave positive

reactions in 3/4 (H-BSE #1) and 4/4 (#2 and #3) replicate wells within 40 h (Fig. 3). At a 10^{-9} dilution, 1 out of 4 replicate wells was positive for two of the H-BSE brain tissue samples, while the third brain sample was negative for all 4 replicates. Using Spearman-Kärber analysis, 50% seeding dose (SD_{50}) titers of $10^{8.20}$ to $10^{8.45}$ SD_{50}/mg of tissue were estimated, which were comparable to the highest titers we have seen with BV rPrP^{Sen} 23–230, M₁₀₉, and most other substrates for prion strains from other host species (47).

H-BSE, L-BSE, and C-BSE prion seeding activity detection using other rPrP^{Sen} substrates. We then tested 11 other rPrP^{Sen} substrates for their relative utility in detecting these bovine prion strains (see Materials and Methods and Fig. 4). All of these substrates detected seeding activity in a 10^{-4} dilution of H-BSE brain homogenate in 4/4 replicate reactions, with average lag phases of 5

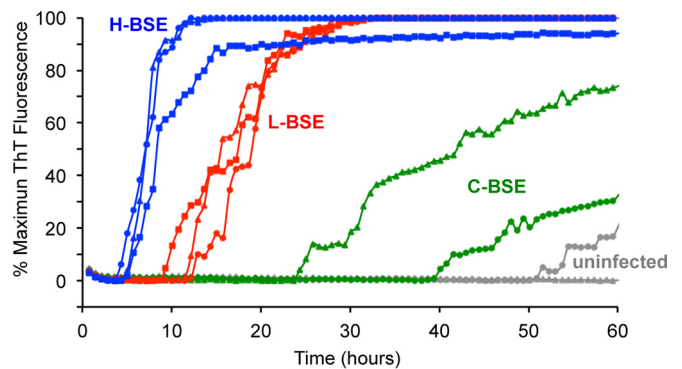


FIG 2 RT-QuIC detection of C-, L-, and H-BSE prion seeding activity using bank vole rPrP^{Sen} 23–230, M₁₀₉. Quadruplicate RT-QuIC reaction mixtures were seeded with 10^{-5} dilutions of brain tissues from uninfected (gray lines, $n = 2$), C-BSE-affected (green lines, $n = 2$), L-BSE-affected (red lines, $n = 3$) and H-BSE-affected (blue lines, $n = 3$) cattle. A final SDS concentration of 0.001% in combination with 300 mM NaCl was used with the BV rPrP^{Sen} 23–230, M₁₀₉ substrate. Similar results were observed in three independent experiments, and representative RT-QuIC data are shown. Thioflavin T fluorescence measurements (the average of four replicate wells; y axis) are plotted as a function of time (hours; x axis).

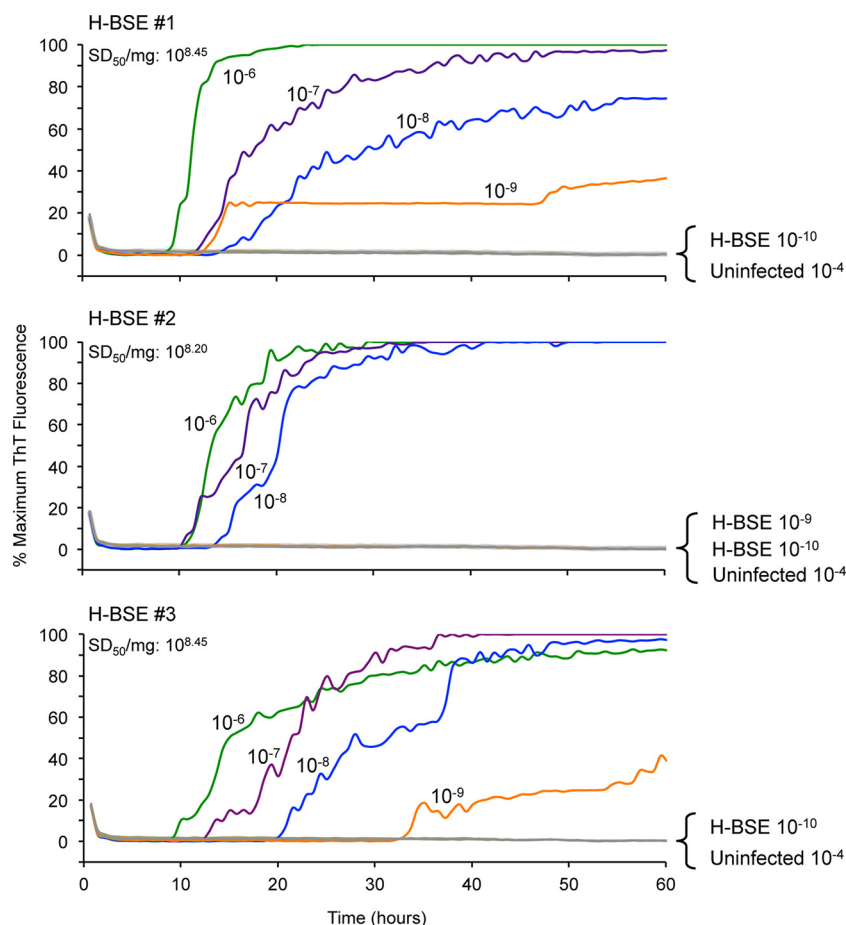


FIG 3 RT-QuIC endpoint dilution analyses of brain tissues from H-BSE-affected cattle using bank vole rPrP^{Scn} 23–230, M₁₀₉. The designated dilution of brain tissue from H-BSE cattle number 1, 2, or 3 and uninfected cattle ($n = 2$) were used to seed RT-QuIC reaction mixtures in the presence of 0.001% SDS and 300 mM NaCl using BV rPrP^{Scn} 23–230, M₁₀₉ as the substrate. Each trace indicates the average fluorescence (y axes) from four replicate wells seeded with the same brain homogenate dilution. Similar results were observed in two independent experiments. The calculated 50% seeding dose (SD_{50}) per mg of brain tissue is indicated for each brain sample tested.

to 20 h, while uninfected brain homogenate gave no positive reactions within 40 h (Fig. 4A to L). The shortest lag phases were observed with those substrates containing the BV sequence. Overall, these results showed that H-BSE brain homogenate was able to seed amyloid formation by 12 different rPrP^{Scn} substrate molecules in RT-QuIC reactions.

Each of these same substrates also detected 10^{-4} dilutions of L-BSE brain homogenates in all replicate reactions (Fig. 4A to L). With a majority of these substrates (BV rPrP^{Scn} 90–230, M₁₀₉; BV rPrP^{Scn} 23–230, I₁₀₉; Hu-BV rPrP^{Scn} 23–230, M₁₀₉; Mo rPrP^{Scn} 23–231; Hu rPrP^{Scn} 23–231, M₁₂₉; Ha rPrP^{Scn} 23–231; and Ha rPrP^{Scn} 90–231), the L-BSE seeds gave longer lag phases than those seen with H-BSE. With BV rPrP^{Scn} 23–230, M₁₀₉ and Hu-BV rPrP^{Scn} 23–230, M₁₀₉ in particular, the L-BSE-seeded reaction mixtures always had a longer lag phase than was observed in simultaneous reaction mixtures seeded with comparable dilutions of H-BSE brain homogenate (Fig. 4A). However, comparable or shorter lag phases were seen for L-BSE with the substrates containing sheep sequence (Fig. 4I to L). The shortest lag phase for L-BSE was seen with the sheep (Sh) ARR sequence (Fig. 4K).

Only half of these various rPrP^{Scn} substrates detected seeding activity in 10^{-4} dilutions of C-BSE within 40 h, and in all cases, the

lag phases were much longer and the mean ThT fluorescence levels weaker, than those observed with comparable dilutions of H-BSE or L-BSE brain homogenates (Fig. 4). Thus, altogether, these results provided evidence that the H-, L-, and C-BSE in these brains differed in their relative abilities to seed amyloid formation by these 12 rPrP^{Scn} substrates.

The strain-dependent differences in RT-QuIC kinetics that we observed with BV rPrP^{Scn} 23–230 and Sh rPrP^{Scn} ARR 25–234 substrates suggested the following potential strategy for discriminating these strains by RT-QuIC: if an unknown bovine sample was positive at a given dilution using the BV substrate, it might contain prion seeds of any one of the three strains. However, if the same dilution were tested concurrently with the Sh rPrP^{Scn} ARR 25–234 substrate, the lag phase should be markedly longer if the unknown were H-BSE, shorter if it were L-BSE, and undetectable if it were C-BSE (Fig. 5). We further tested this diagnostic algorithm on brain samples from cattle clinically affected with each of the BSE strains (3 cattle per strain) (Fig. 6). Three dilutions (10^{-3} , 10^{-4} , and 10^{-5}) of each brain sample were tested using the BV rPrP^{Scn} 23–230 and Sh rPrP^{Scn} ARR 25–234 substrates. Consistent with the above-described results, all of the brain samples gave positive reactions with the BV rPrP^{Scn} 23–230 substrate (darker

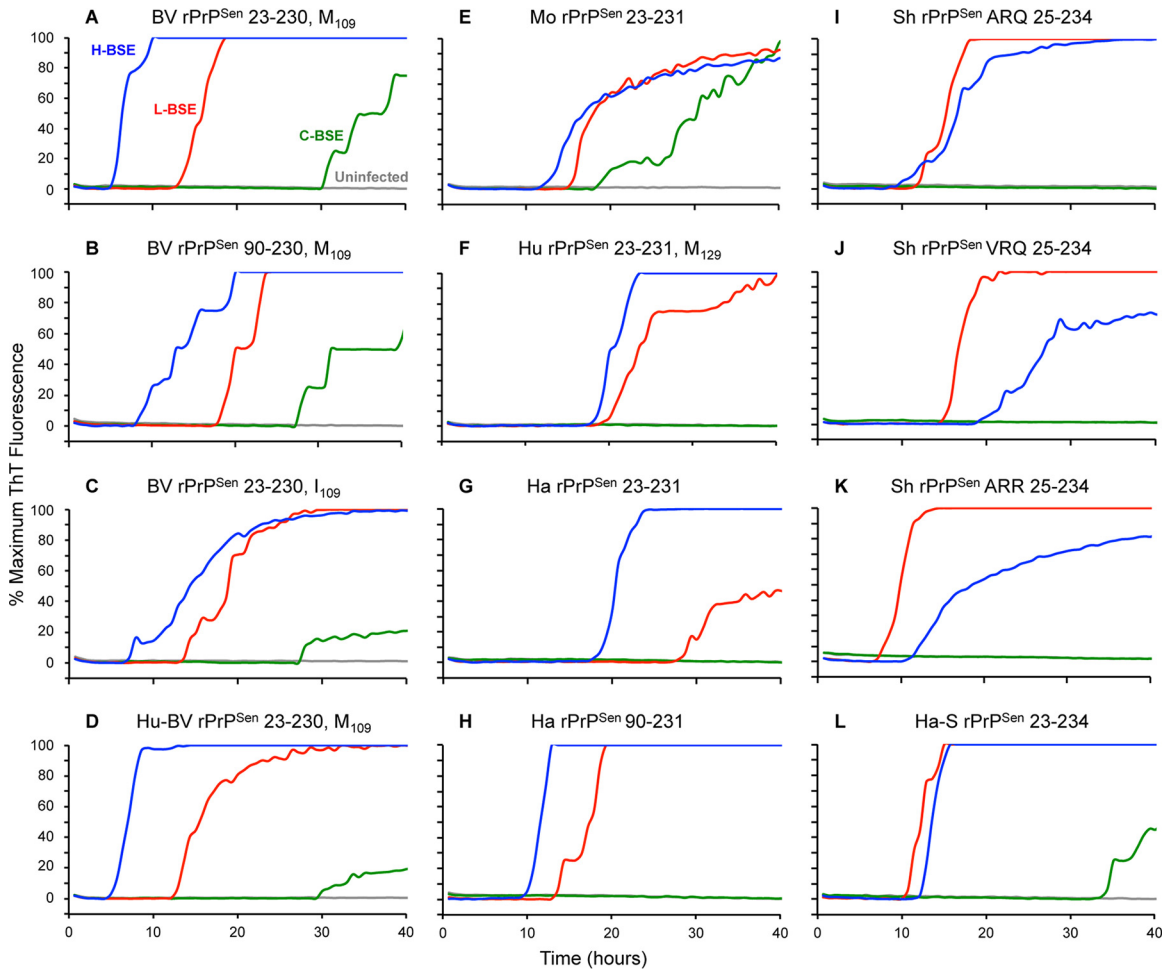


FIG 4 RT-QuIC detection of C-, L-, and H-BSE prion seeding activity in brain samples using multiple rPrP^{Sen} substrates. Quadruplicate RT-QuIC reaction mixtures were seeded with 10^{-4} brain tissue dilutions from uninfected (gray lines), C-BSE-affected (green lines), L-BSE-affected (red lines), and H-BSE-affected (blue lines) cattle in the presence of 0.001% SDS. A final concentration of either 300 mM NaCl (BV rPrP^{Sen} 23–230, M₁₀₉ [A], BV rPrP^{Sen} 90–230, M₁₀₉ [B], BV rPrP^{Sen} 23–230, I₁₀₉ [C], Hu-BV rPrP^{Sen} 23–230, M₁₀₉ [D], Ha rPrP^{Sen} 23–231 [G], Ha rPrP^{Sen} 90–231 [H], Sh rPrP^{Sen} ARQ 25–234 [I], VRQ 25–234 [J], ARR 25–234 [K], and Ha-S rPrP^{Sen} 23–234 [L]) or 130 mM NaCl (Mo rPrP^{Sen} 23–231 [E] and Hu rPrP^{Sen} 23–231 [F]) was used. Traces from representative RT-QuIC experiments are shown as the average of ThT fluorescence (*y* axes) from four replicate wells.

colors), while only the H-BSE and L-BSE brain samples gave positive reactions with the Sh rPrP^{Sen} ARR 25–234 substrate (lighter colors). Uninfected brains were negative for all replicate reactions for at least 50 h. Also, at each dilution of each H-BSE brain, the lag phase with the Sh rPrP^{Sen} ARR 25–234 substrate was approximately double that obtained with the BV rPrP^{Sen} 23–230 substrate. In contrast, for each dilution of the L-BSE brain samples, the lag phase with the Sh rPrP^{Sen} ARR 25–234 substrate was shorter than that with the BV substrate. Thus, these results provided evidence that C-, L-, and H-BSE can be discriminated based on relative reactivities and lag phases obtained using the BV rPrP^{Sen} 23–230 and Sh rPrP^{Sen} ARR 25–234 substrates.

To further test our ability to discriminate the BSE strains by RT-QuIC using the above-described algorithm, we retested all of the available H-BSE ($n = 3$), L-BSE ($n = 3$), and C-BSE ($n = 3$) samples described above after the samples were blinded by a colleague not otherwise involved in this study. In all cases, the correct strain identification was made as long as brain homogenate dilutions of 10^{-3} to 10^{-5} were used. With more extreme dilutions, the

greater variability in lag phase, which is typically seen in RT-QuIC reaction mixtures seeded with low levels of prion seeding activity (41), sometimes confounded strain identification (data not shown). Furthermore, we found that it was important to use a single plate to compare the relative kinetics with BV rPrP^{Sen} 23–230 and Sh rPrP^{Sen} ARR 25–234 substrates for a given test sample, along with positive controls of each strain. This precaution was needed because, as we have seen previously with other RT-QuIC assays, seemingly subtle differences in reaction conditions that occur between experiments and fluorimeters can influence lag phases to the extent that they also confound strain identification.

Discrimination of H-BSE from L-BSE and C-BSE by immunoblotting of RT-QuIC products. Another RT-QuIC-based approach to discriminating prion strains is the comparison of the profile of PK-resistant products of RT-QuIC reactions using the BV rPrP^{Sen} 23–230, M₁₀₉ substrate by Western blotting (47). We tested this approach by comparing the products of reaction mixtures seeded with brain samples from H-, L-, and C-BSE-affected cattle (Fig. 7A). H- and C-BSE-seeded reaction products were dif-

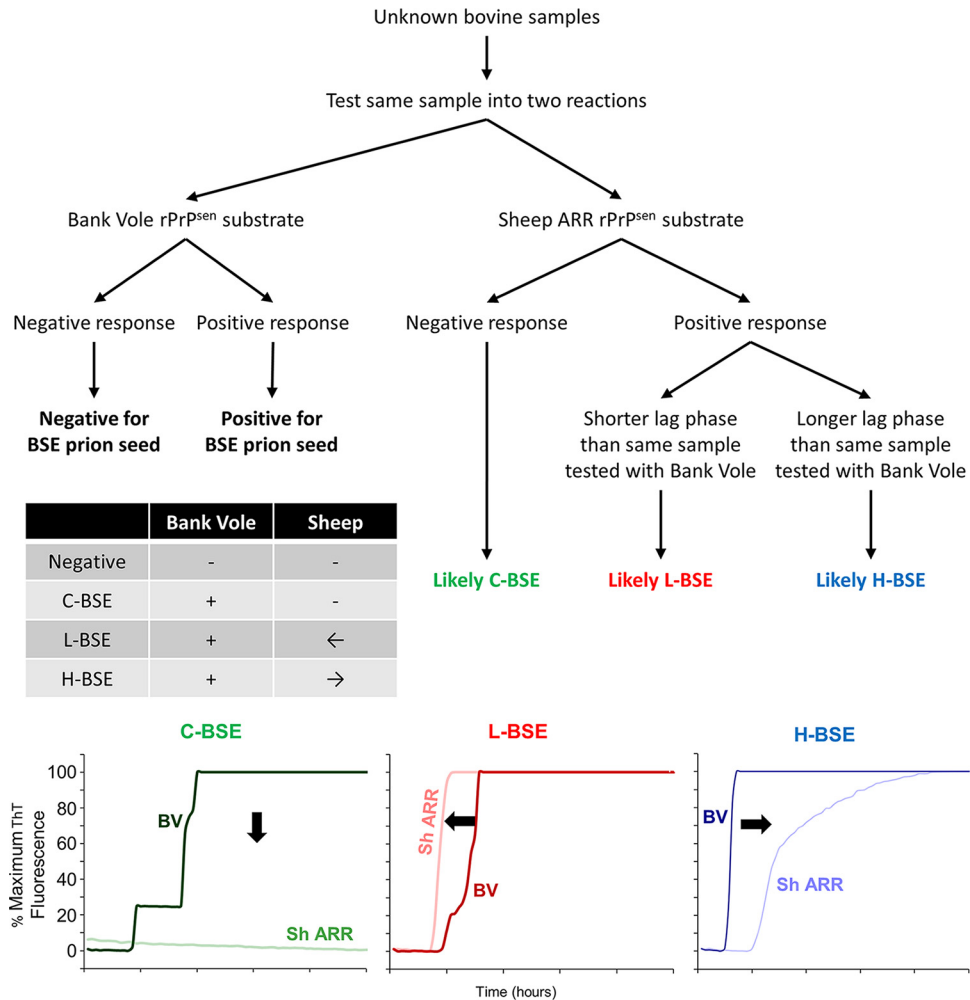


FIG 5 Schematic for RT-QuIC-based discrimination for C-, L-, and H-BSE. A decision tree is shown illustrating the steps for RT-QuIC discrimination of C-, L-, and H-type BSE strains (green, red and blue, respectively). The table summarizes the possible outcomes of RT-QuIC testing using both BV 23–230, M₁₀₉ and Sh ARR 25–234 rPrP^{Sen} in the same plate. The graphs represent three examples of RT-QuIC kinetics observed using BV rPrP^{Sen} 23–230, M₁₀₉ and Sh ARR 25–234 rPrP^{Sen}. The arrows in the table and the graphs indicate the shift in lag phase using Sh ARR relative to BV rPrP^{Sen}.

difficult to distinguish from one another, with each having a predominant 10-kDa band and a weaker band or a diffuse smear at ~12 kDa (Fig. 7B). In contrast, the L-BSE-seeded products had stronger relative ratios of the intensity of the 12-kDa band to that of the 10-kDa band ($P < 0.001$, t test) compared to C- and H-BSE-seeded products (Fig. 7B). Thus, these relative banding patterns might provide an additional means of discriminating L- and H-BSE and be helpful in future analyses to confirm BSE strain identifications.

Detection of prion seeding activity in CSF of H- and L-BSE-infected cattle. Because prion seeding activity has been detected in CSF samples from prion-infected humans, sheep, rodents, and deer (42, 52–56), we tested whether the same is true in BSE-infected cattle. We tested 20 μ l of neat CSF samples from 2 C-BSE, 4 L-BSE, 2 H-BSE-affected cattle and 2 uninfected cattle using either the BV rPrP^{Sen} 23–230, M₁₀₉, BV rPrP^{Sen} 90–230, M₁₀₉, or Ha rPrP^{Sen} 90–231 substrate. Both H-BSE cattle (Fig. 8, blue) gave positive reaction products in 2/2 replicate reactions performed with BV rPrP^{Sen} 23–230, M₁₀₉ and 2/3 or 3/3 reactions with Ha rPrP^{Sen} 90–231 (Fig. 8A and C, respectively). However, only one of the H-BSE cattle was clearly positive, relative to the uninfected

controls, using the BV rPrP^{Sen} 90–230, M₁₀₉ substrate (Fig. 8B). CSF samples from three of four L-BSE cattle (Fig. 8, red) gave 3/3 positive replicate reaction products with the Ha rPrP^{Sen} 90–231 substrate, while the fourth reaction was negative (Fig. 8C). The other two substrates appeared to be less sensitive for detecting L-BSE in CSF (Fig. 8A and B). Finally, no positive reaction products were detected in CSF samples from two C-BSE cattle with any of the three substrates (Fig. 8A and C). Collectively, these results indicate preliminarily that the Ha rPrP^{Sen} 90–231 substrate was the most effective in detecting both H- and L-BSE in bovine CSF samples and that prion seeding activity was detectable in at least some of the H- and L-BSE-infected cattle but not in C-BSE-infected or uninfected cattle. These results support the concept that the most suitable rPrP^{Sen} substrate may be different depending on the bodily fluids or tissues being tested.

DISCUSSION

The C-BSE epidemic in cattle and its causation of vCJD in humans have had serious impacts on both the cattle industry and human health. The incidence of C-BSE has virtually been eliminated by

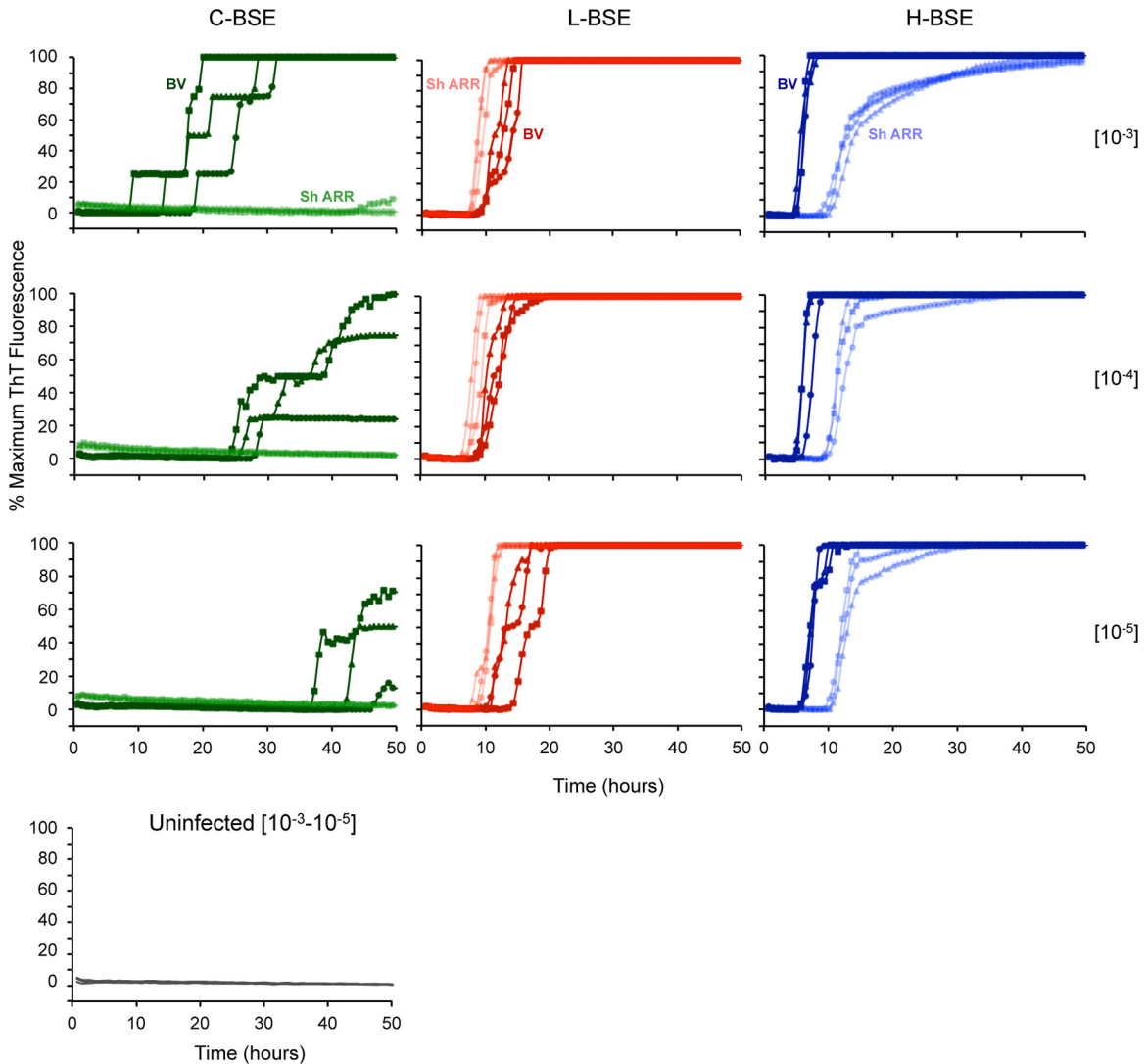


FIG 6 Detection and discrimination of C-, L-, and H-BSE prior seeding activity by RT-QuIC using BV rPrP^{Scn} 23–230, M₁₀₉ and Sh rPrP^{Scn} ARR 25–234. Serial dilutions of brain homogenates (10^{-3} , 10^{-4} , and 10^{-5}) from three C-BSE-, three L-BSE-, and three H-BSE-affected cattle and one uninfected animal were tested by RT-QuIC. The same brain homogenate dilutions (circles, triangles, and squares indicate individual animals) were used to seed reaction mixtures with either BV rPrP^{Scn} 23–230, M₁₀₉ (dark shades of green, red, and blue) or Sh rPrP^{Scn} ARR 25–234 (light shades of green, red, and blue). Representative data from at least two independent experiments are shown. The traces are the average fluorescence values (*y* axes) results from of four replicate wells.

effective, albeit costly, measures to minimize its propagation within cattle and zoonotic transmission from cattle into humans. However, the recent appendix-based evidence for widespread subclinical prion infections of humans (18) raises the specter of longer-term consequences of the C-BSE epidemic. At the same time, the likelihood that atypical forms of BSE can arise spontaneously in cattle, as apparently occurs with sporadic CJD in humans, suggests that continuous surveillance for H- and L-BSE, coupled with appropriate containment measures, will be required to prevent outbreaks in cattle and mitigate risks to humans and other species. The current commercially available rapid tests that are approved for postmortem BSE surveillance are indeed practical and effective at identifying the many problematic cases of classical or atypical BSE-infected cattle that might indicate a focus of bovine prion disease or threaten the human food supply. How-

ever, these tests are not sensitive enough to detect all potential sources of BSE infection, because they are orders-of-magnitude-less sensitive than bioassays for BSE infectivity (33–36). The sandwich CDI assay described by Safar and colleagues (35) is nearly as sensitive as the best animal bioassays for C-BSE but, to our knowledge, has not been described for the atypical strains of BSE. Thus, the effectiveness of BSE testing would likely be aided by our demonstration here of highly sensitive and practical tests for the detection and discrimination of each of the established strains of BSE in cattle.

As noted above, our previous studies demonstrated RT-QuIC assays capable of sensitive detection and discrimination of C-BSE and L-BSE using various rPrP^{Scn} substrates (40, 47). Here, we describe an ultrasensitive RT-QuIC assay that also detects H-BSE prion seeding activity in H-BSE brain homoge-

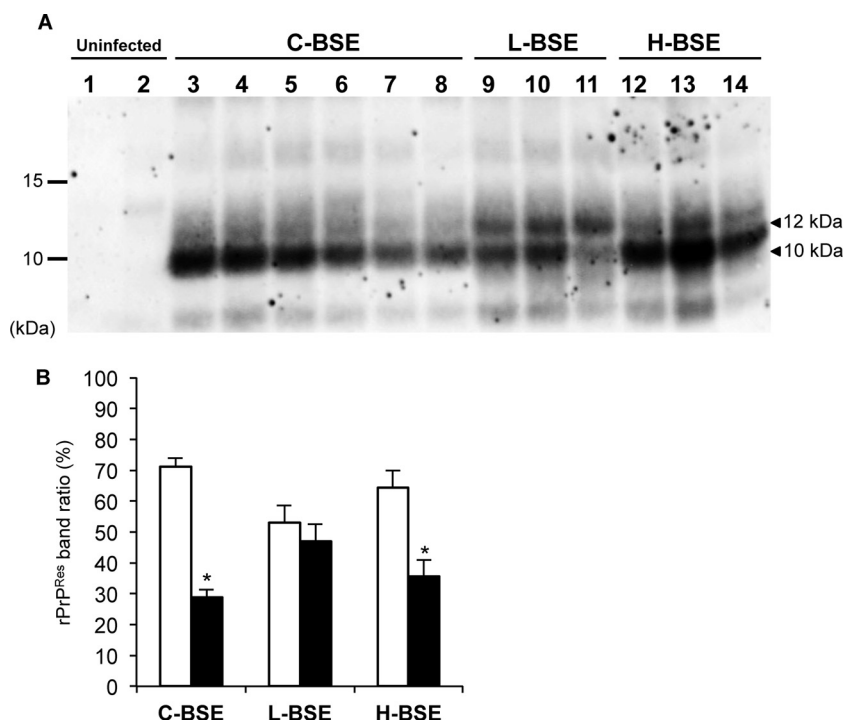


FIG 7 Western blot analysis of BV rPrP^{Res} products from RT-QuIC reaction mixtures seeded with C-, L-, and H-BSE strains. Reaction products were digested with 10 μ g/ml PK at 37°C for 1 h. BV rPrP^{Res} conversion products were detected using C-terminal antiserum R20 (hamster PrP epitope residues 218 to 231). (A) BV rPrP^{Res} conversion products from reaction mixtures seeded with uninfected (lanes 1 and 2, $n = 2$), C-BSE (lanes 3 to 8, $n = 6$), L-BSE (lanes 9 to 11, $n = 3$), or H-BSE (lanes 12 to 14, $n = 3$) brain tissue dilutions. RT-QuIC and immunoblotting analyses were performed at least twice for each brain sample with similar results. The molecular mass markers are shown on the left in kilodaltons. (B) ImageQuant TL software densitometry quantification of the relative intensity of the lower (10 kDa, white bars) and the upper (12 kDa, black bars) bands of BV rPrP^{Res} products generated by seeding with C-, L-, or H-BSE brain homogenate dilutions. The results are represented as the means \pm standard deviations (SD) from the results from two independent experiments in which seeding activity from each of the three BSE strains was detected. The asterisks indicate statistically significant differences in the signal intensity of the 12-kDa band between L-BSE and other BSE strains ($P < 0.001$, Student's *t* test).

nate dilutions of 10^{-5} within 5 to 10 h and dilutions of as little as 10^{-8} within 24 h. To our knowledge, the corresponding sensitivities of animal bioassays and PMCA for the atypical BSE strains have not yet been described, but for C-BSE, our RT-QuIC tests appear to be at least as sensitive as bioassays and nearly as sensitive as PMCA (37–39). With sensitivities that are orders-of-magnitude greater than the commercially available rapid immunochemical tests, our RT-QuIC tests should be able to detect BSE in a larger proportion of cattle and in tissue specimens with much lower, but still potentially infectious, levels of contamination. This improves the likelihood that, as is the case for sporadic CJD (sCJD) in humans (42, 49, 52, 54), antemortem diagnostic tests can be developed that are based on analyses of tissue or fluids that can be obtained from live cattle. Here, we have demonstrated the detection of prion seeding activity in CSF samples from cattle infected with H-BSE and L-BSE but not C-BSE (Fig. 7); however, CSF is not likely to be practical as an antemortem diagnostic specimen source for cattle, so testing of other more-accessible tissue specimens is warranted. As noted above, RT-QuIC assays can be quantitative (41, 57–60), facilitating assessments of the relative amounts of prion seeding activity in various diagnostic specimens and tissues that might end up in the food supply (61).

Through comparisons of H-, L-, and C-BSE reactivities with 12 different recombinant PrP substrates, we also demonstrate a means to clearly discriminate each of three major bovine prion

strains. In practice, test samples should be run simultaneously with the BV rPrP^{Sen} 23–230 and sheep rPrP^{Sen} ARR 25–234 substrates in the same plate, allowing detection and strain discrimination in one assay. In such an assay, it would be advisable to include positive-control standards of each strain to allow direct internal comparisons to be made. Additionally, our data indicate that strain identification by the algorithm we described above (and see Fig. 5) works for dilutions of 10^{-3} to 10^{-5} of brain tissue from clinically affected cattle but not more extreme dilutions that are closer to the detection limit of the assay. A possible implication of this observation is that BSE strain discrimination between H- and L-BSE might not be feasible with RT-QuIC alone using test samples that have reduced concentrations of prion seeding activity. Such samples might include brain tissue from preclinical BSE-infected cattle or non-central nervous system (CNS) tissues with lower levels of seeding activity.

In conclusion, RT-QuIC assays are less labor-intensive, time-consuming, and technically demanding than comparably sensitive PMCA tests for BSE (37, 38), which require sonication rather than shaking and Western blotting rather than fluorescence as a readout. Thus, as of this writing, our currently described RT-QuIC assays for BSE appear to be the most practical means for detecting all infectious levels of the three major BSE strains. Furthermore, when brain samples (at least) contain sufficient seed

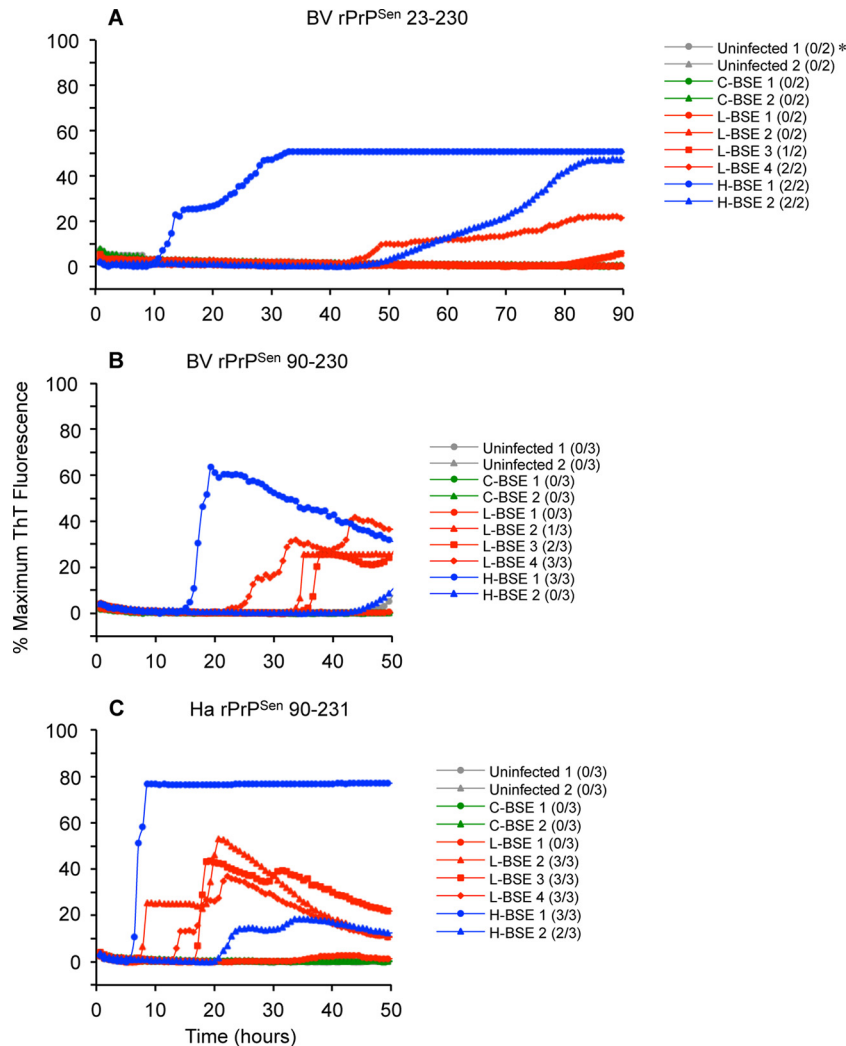


FIG 8 RT-QuIC analysis of CSF from C-, L-, and H-BSE-positive cattle using BV rPrP^{Sen} 23–230, M₁₀₉, BV rPrP^{Sen} 90–230, M₁₀₉, and hamster rPrP^{Sen} 90–231. CSF samples from two C-BSE-, four L-BSE-, and two H-BSE-affected cattle and two uninfected cattle were tested by RT-QuIC. BV rPrP^{Sen} 90–230, M₁₀₉ (B), and Ha rPrP^{Sen} 90–231 (C) were used as substrates in the presence of 0.002% SDS and 300 mM NaCl. The reaction mixtures were incubated at 42°C (BV rPrP^{Sen} 23–230, M₁₀₉) or 55°C (BV rPrP^{Sen} 90–230, M₁₀₉ and Ha rPrP^{Sen} 90–231). The traces are the average fluorescence values (γ axes) of replicate wells. * The fractions indicate the number of positive wells out of the total number of replicate reactions for each sample.

concentrations, RT-QuIC can discriminate these strains from one another.

ACKNOWLEDGMENTS

We thank Shigeo Fukuda for providing the BSE samples. We thank Ritsuko Miwa, Naoko Tabeta, Junko Yamada, and Gregory Raymond for technical assistance and Karin Peterson and Roger Moore for the critical review of the manuscript.

FUNDING INFORMATION

A research fellowship from NARO provided funding to Kentaro Masujin. Alliance Biosecure Foundation under the aegis of the Fondation pour la Recherche Medicale provided funding to Byron Caughey. The Intramural Research Program of the National Institute of Allergy and Infectious Diseases (DIR, NIAID) provided funding to Byron Caughey.

This work was supported in part by the Intramural Research Program of the NIAID, by the Alliance Biosecure Foundation under the aegis of the

Fondation pour la Recherche Médicale (FABS 201401), and by a research fellowship from NARO to K. Masujin.

REFERENCES

- Kraus A, Groveman BR, Caughey B. 2013. Prions and the potential transmissibility of protein misfolding diseases. *Annu Rev Microbiol* 67: 543–564. <http://dx.doi.org/10.1146/annurev-micro-092412-155735>.
- Telling GC. 2013. The importance of prions. *PLoS Pathog* 9:e1003090. <http://dx.doi.org/10.1371/journal.ppat.1003090>.
- Prusiner SB. 1998. Prions. *Proc Natl Acad Sci U S A* 95:13363–13383. <http://dx.doi.org/10.1073/pnas.95.23.13363>.
- Castilla J, Saá P, Hetz C, Soto C. 2005. *In vitro* generation of infectious scrapie prions. *Cell* 121:195–206. <http://dx.doi.org/10.1016/j.cell.2005.02.011>.
- Silveira JR, Raymond GJ, Hughson AG, Race RE, Sim VL, Hayes SF, Caughey B. 2005. The most infectious prion protein particles. *Nature* 437:257–261. <http://dx.doi.org/10.1038/nature03989>.
- Deleault NR, Harris BT, Rees JR, Supattapone S. 2007. Formation of native prions from minimal components *in vitro*. *Proc Natl Acad Sci U S A* 104:9741–9746. <http://dx.doi.org/10.1073/pnas.0702662104>.

7. Legname G, Baskakov IV, Nguyen HO, Riesner D, Cohen FE, DeArmond SJ, Prusiner SB. 2004. Synthetic mammalian prions. *Science* 305: 673–676. <http://dx.doi.org/10.1126/science.1100195>.
8. Wang F, Wang X, Yuan C-G, Ma J. 2010. Generating a prion with bacterially expressed recombinant prion protein. *Science* 327:1132–1135. <http://dx.doi.org/10.1126/science.1183748>.
9. Kim JI, Cali I, Surewicz K, Kong Q, Raymond GJ, Atarashi R, Race B, Qing L, Gambetti P, Caughey B, Surewicz WK. 2010. Mammalian prions generated from bacterially expressed prion protein in the absence of any mammalian cofactors. *J Biol Chem* 285:14083–14087. <http://dx.doi.org/10.1074/jbc.C110.113464>.
10. Makarava N, Kovacs GG, Bocharova O, Savtchenko R, Alexeeva I, Budka H, Rohwer RG, Baskakov IV. 2010. Recombinant prion protein induces a new transmissible prion disease in wild-type animals. *Acta Neuropathol* 119:177–187. <http://dx.doi.org/10.1007/s00401-009-0633-x>.
11. Bruce ME. 2003. TSE strain variation. *Br Med Bull* 66:99–108. <http://dx.doi.org/10.1093/bmb/66.1.99>.
12. Bessen RA, Marsh RF. 1994. Distinct PrP properties suggest the molecular basis of strain variation in transmissible mink encephalopathy. *J Virol* 68:7859–7868.
13. Bessen RA, Kocisko DA, Raymond GJ, Nandan S, Lansbury PT, Jr, Caughey B. 1995. Non-genetic propagation of strain-specific phenotypes of scrapie prion protein. *Nature* 375:698–700. <http://dx.doi.org/10.1038/375698a0>.
14. Safar J, Wille H, Itri V, Groth D, Serban H, Torchia M, Cohen FE, Prusiner SB. 1998. Eight prion strains have PrP(Sc) molecules with different conformations. *Nat Med* 4:1157–1165. <http://dx.doi.org/10.1038/2654>.
15. Baron GS, Hughson AG, Raymond GJ, Offerdahl DK, Barton KA, Raymond LD, Dorward DW, Caughey B. 2011. Effect of glycans and the glycosphosphatidylinositol anchor on strain dependent conformations of scrapie prion protein: improved purifications and infrared spectra. *Biochemistry* 50:4479–4490. <http://dx.doi.org/10.1021/bi2003907>.
16. Parchi P, de Boni L, Saverioni D, Cohen ML, Ferrer I, Gambetti P, Gelpi E, Giaccone G, Hauw JJ, Hofberger R, Ironside JW, Jansen C, Kovacs GG, Rozemuller A, Seilhean D, Tagliavini F, Giese A, Kretschmar HA. 2012. Consensus classification of human prion disease histotypes allows reliable identification of molecular subtypes: an inter-rater study among surveillance centres in Europe and USA *Acta Neuropathol* 124:517–529.
17. Bradley R, Wilesmith JW. 1993. Epidemiology and control of bovine spongiform encephalopathy (BSE). *Br Med Bull* 49:932–959.
18. Gill ON, Spencer Y, Richard-Loendt A, Kelly C, Dabaghian R, Boyes L, Linehan J, Simmons M, Webb P, Bellerby P, Andrews N, Hilton DA, Ironside JW, Beck J, Poulter M, Mead S, Brandner S. 2013. Prevalent abnormal prion protein in human appendixes after bovine spongiform encephalopathy epizootic: large scale survey. *BMJ* 347:f5675. <http://dx.doi.org/10.1136/bmj.f5675>.
19. Casalone C, Zanusso G, Acutis P, Ferrari S, Capucci L, Tagliavini F, Monaco S, Caramelli M. 2004. Identification of a second bovine amyloidotic spongiform encephalopathy: molecular similarities with sporadic Creutzfeldt-Jakob disease. *Proc Natl Acad Sci U S A* 101:3065–3070. <http://dx.doi.org/10.1073/pnas.0305777101>.
20. Baron T, Vulin J, Biacabe AG, Lakhdar L, Verchere J, Torres JM, Bencsik A. 2011. Emergence of classical BSE strain properties during serial passages of H-BSE in wild-type mice. *PLoS One* 6:e15839. <http://dx.doi.org/10.1371/journal.pone.0015839>.
21. Torres JM, Andreoletti O, Lacroux C, Prieto I, Lorenzo P, Larska M, Baron T, Espinosa JC. 2011. Classical bovine spongiform encephalopathy by transmission of H-type prion in homologous prion protein context. *Emerging Infect Dis* 17:1636–1644. <http://dx.doi.org/10.3201/eid1709.101403>.
22. Biacabe AG, Laplanche JL, Ryder S, Baron T. 2004. Distinct molecular phenotypes in bovine prion diseases. *EMBO Rep* 5:110–115. <http://dx.doi.org/10.1038/sj.embor.7400054>.
23. Windl O, Dawson M. 2012. Animal prion diseases. *Subcell Biochem* 65:497–516. http://dx.doi.org/10.1007/978-94-007-5416-4_18.
24. Brown P, McShane LM, Zanusso G, Detwiler L. 2006. On the question of sporadic or atypical bovine spongiform encephalopathy and Creutzfeldt-Jakob disease. *Emerging Infect Dis* 12:1816–1821. <http://dx.doi.org/10.3201/eid1212.060965>.
25. Fukuda S, Iwamaru Y, Imamura M, Masujin K, Shimizu Y, Matsuura Y, Shu Y, Kurachi M, Kasai K, Murayama Y, Onoe S, Hagiwara K, Sata T, Mohri S, Yokoyama T, Okada H. 2009. Intraspecies transmission of L-type-like bovine spongiform encephalopathy detected in Japan. *Microbiol Immunol* 53:704–707. <http://dx.doi.org/10.1111/j.1348-0421.2009.00169.x>.
26. Lombardi G, Casalone C, A DA, Gelmetti D, Torcoli G, Barbieri I, Corona C, Fasoli E, Farinazzo A, Fiorini M, Gelati M, Iulini B, Tagliavini F, Ferrari S, Caramelli M, Monaco S, Capucci L, Zanusso G. 2008. Intraspecies transmission of BASE induces clinical dullness and amyotrophic changes. *PLoS Pathog* 4:e1000075. <http://dx.doi.org/10.1371/journal.ppat.1000075>.
27. Buschmann A, Gretzschel A, Biacabe AG, Schiebel K, Corona C, Hoffmann C, Eiden M, Baron T, Casalone C, Groschup MH. 2006. Atypical BSE in Germany—proof of transmissibility and biochemical characterization. *Vet Microbiol* 117:103–116. <http://dx.doi.org/10.1016/j.vetmic.2006.06.016>.
28. Masujin K, Shu Y, Yamakawa Y, Hagiwara K, Sata T, Matsuura Y, Iwamaru Y, Imamura M, Okada H, Mohri S, Yokoyama T. 2008. Biological and biochemical characterization of L-type-like bovine spongiform encephalopathy (BSE) detected in Japanese black beef cattle. *Prion* 2:123–128. <http://dx.doi.org/10.4161/pri.2.3.7437>.
29. Kong Q, Zheng M, Casalone C, Qing L, Huang S, Chakraborty B, Wang P, Chen F, Cali I, Corona C, Martucci F, Iulini B, Acutis P, Wang L, Liang J, Wang M, Li X, Monaco S, Zanusso G, Zou WQ, Caramelli M, Gambetti P. 2008. Evaluation of the human transmission risk of an atypical bovine spongiform encephalopathy prion strain. *J Virol* 82:3697–3701. <http://dx.doi.org/10.1128/JVI.02561-07>.
30. Okada H, Masujin K, Iwamaru Y, Imamura M, Matsuura Y, Mohri S, Czub S, Yokoyama T. 2011. Experimental transmission of H-type bovine spongiform encephalopathy to bovinized transgenic mice. *Vet Pathol* 48: 942–947. <http://dx.doi.org/10.1177/0300985810382672>.
31. Bencsik A, Leboivre M, Debeer S, Aufauvre C, Baron T. 2013. Unique properties of the classical bovine spongiform encephalopathy strain and its emergence from H-type bovine spongiform encephalopathy substantiated by VM transmission studies. *J Neuropathol Exp Neurol* 72:211–218. <http://dx.doi.org/10.1097/NEN.0b013e318285c7f9>.
32. Wilson R, Dobie K, Hunter N, Casalone C, Baron T, Barron RM. 2013. Presence of subclinical infection in gene-targeted human prion protein transgenic mice exposed to atypical bovine spongiform encephalopathy. *J Gen Virol* 94:2819–2827. <http://dx.doi.org/10.1099/vir.0.052738-0>.
33. Gray JG, Dudas S, Graham C, Czub S. 2012. Performance analysis of rapid diagnostic tests on atypical bovine spongiform encephalopathy. *J Vet Diagn Invest* 24:976–980. <http://dx.doi.org/10.1177/1040638712455325>.
34. Meloni D, Davide A, Langeveld JP, Varello K, Casalone C, Corona C, Balkema-Buschmann A, Groschup MH, Ingravalle F, Bozzetta E. 2012. EU-approved rapid tests for bovine spongiform encephalopathy detect atypical forms: a study for their sensitivities. *PLoS One* 7:e43133. <http://dx.doi.org/10.1371/journal.pone.0043133>.
35. Safar JG, Scott M, Monaghan J, Deering C, Didorenko S, Vergara J, Ball H, Legname G, Leclerc E, Solforosi L, Serban H, Groth D, Burton DR, Prusiner SB, Williamson RA. 2002. Measuring prions causing bovine spongiform encephalopathy or chronic wasting disease by immunoassays and transgenic mice. *Nat Biotechnol* 20:1147–1150. <http://dx.doi.org/10.1038/nbt748>.
36. Buschmann A, Groschup MH. 2005. Highly bovine spongiform encephalopathy-sensitive transgenic mice confirm the essential restriction of infectivity to the nervous system in clinically diseased cattle. *J Infect Dis* 192:934–942. <http://dx.doi.org/10.1086/431602>.
37. Murayama Y, Yoshioka M, Masujin K, Okada H, Iwamaru Y, Imamura M, Matsuura Y, Fukuda S, Onoe S, Yokoyama T, Mohri S. 2010. Sulfated dextrans enhance *in vitro* amplification of bovine spongiform encephalopathy PrP(Sc) and enable ultrasensitive detection of bovine PrP(Sc). *PLoS One* 5:e013152. <http://dx.doi.org/10.1371/journal.pone.0013152>.
38. Murayama Y, Masujin K, Imamura M, Ono F, Shibata H, Tobiume M, Yamamura T, Shimozaki N, Terao K, Yamakawa Y, Sata T. 2014. Ultrasensitive detection of PrP(Sc) in the cerebrospinal fluid and blood of macaques infected with bovine spongiform encephalopathy prion. *J Gen Virol* 95:2576–2588. <http://dx.doi.org/10.1099/vir.0.066225-0>.
39. Lacroux C, Comoy E, Moudjou M, Perret-Liaudet A, Lugan S, Litaise C, Simmons H, Jas-Duval C, Lantier I, Beringue V, Groschup M, Fichet G, Costes P, Streichenberger N, Lantier F, Deslys JP, Vilette D, Andreoletti O. 2014. Preclinical detection of variant CJD

- and BSE prions in blood. *PLoS Pathog* 10:e1004202. <http://dx.doi.org/10.1371/journal.ppat.1004202>.
40. Orru CD, Favole A, Corona C, Mazza M, Manca M, Groveman BR, Hughson AG, Acutis PL, Caramelli M, Zanusso G, Casalone C, Caughey B. 2015. Detection and discrimination of classical and atypical L-type bovine spongiform encephalopathy by real-time quaking-induced conversion. *J Clin Microbiol* 53:1115–1120. <http://dx.doi.org/10.1128/JCM.02906-14>.
 41. Wilham JM, Orrú CD, Bessen RA, Atarashi R, Sano K, Race B, Meade-White KD, Taubner LM, Timmes A, Caughey B. 2010. Rapid end-point quantitation of prion seeding activity with sensitivity comparable to bioassays. *PLoS Pathog* 6:e1001217. <http://dx.doi.org/10.1371/journal.ppat.1001217>.
 42. Atarashi R, Satoh K, Sano K, Fuse T, Yamaguchi N, Ishibashi D, Matsubara T, Nakagaki T, Yamanaka H, Shirabe S, Yamada M, Mizusawa H, Kitamoto T, Klug G, McGlade A, Collins SJ, Nishida N. 2011. Ultrasensitive human prion detection in cerebrospinal fluid by real-time quaking-induced conversion. *Nat Med* 17:175–178. <http://dx.doi.org/10.1038/nm.2294>.
 43. Okada H, Iwamaru Y, Imamura M, Masujin K, Matsuura Y, Shimizu Y, Kasai K, Mohri S, Yokoyama T, Czub S. 2011. Experimental H-type bovine spongiform encephalopathy characterized by plaques and glial- and stellate-type prion protein deposits. *Vet Res* 42:79. <http://dx.doi.org/10.1186/1297-9716-42-79>.
 44. Fukuda S, Onoe S, Nikaido S, Fujii K, Kageyama S, Iwamaru Y, Imamura M, Masujin K, Matsuura Y, Shimizu Y, Kasai K, Yoshioka M, Murayama Y, Mohri S, Yokoyama T, Okada H. 2012. Neuroanatomical distribution of disease-associated prion protein in experimental bovine spongiform encephalopathy in cattle after intracerebral inoculation. *Jpn J Infect Dis* 65:37–44.
 45. Shimizu Y, Kaku-Ushiki Y, Iwamaru Y, Muramoto T, Kitamoto T, Yokoyama T, Mohri S, Tagawa Y. 2010. A novel anti-prion protein monoclonal antibody and its single-chain fragment variable derivative with ability to inhibit abnormal prion protein accumulation in cultured cells. *Microbiol Immunol* 54:112–121. <http://dx.doi.org/10.1111/j.1348-0421.2009.00190.x>.
 46. Groveman BR, Kraus A, Raymond LD, Dolan MA, Anson KJ, Dorward DW, Caughey B. 2015. Charge neutralization of the central lysine cluster in prion protein (PrP) promotes PrP(Sc)-like folding of recombinant PrP amyloids. *J Biol Chem* 290:1119–1128. <http://dx.doi.org/10.1074/jbc.M114.619627>.
 47. Orrú CD, Groveman BR, Raymond LD, Hughson AG, Nonno R, Zou W, Ghetti B, Gambetti P, Caughey B. 2015. Bank vole prion protein as an apparently universal substrate for RT-QuIC-based detection and discrimination of prion strains. *PLoS Pathog* 11:e1004983. <http://dx.doi.org/10.1371/journal.ppat.1004983>.
 48. Sano K, Satoh K, Atarashi R, Takashima H, Iwasaki Y, Yoshida M, Sanjo N, Murai H, Mizusawa H, Schmitz M, Zerr I, Kim YS, Nishida N. 2013. Early detection of abnormal prion protein in genetic human prion diseases now possible using real-time QUIC assay. *PLoS One* 8:e54915. <http://dx.doi.org/10.1371/journal.pone.0054915>.
 49. Orrú CD, Bongianini M, Tonoli G, Ferrari S, Hughson AG, Groveman BR, Fiorini M, Pocchiari M, Monaco S, Caughey B, Zanusso G. 2014. A test for Creutzfeldt-Jakob disease using nasal brushings. *N Engl J Med* 371:519–529. <http://dx.doi.org/10.1056/NEJMoa1315200>.
 50. Caughey B, Raymond GJ, Ernst D, Race RE. 1991. N-terminal truncation of the scrapie-associated form of PrP by lysosomal protease(s): implications regarding the site of conversion of PrP to the protease-resistant state. *J Virol* 65:6597–6603.
 51. Vascellari S, Orru CD, Hughson AG, King D, Barron R, Wilham JM, Baron GS, Race B, Pani A, Caughey B. 2012. Prion seeding activities of mouse scrapie strains with divergent PrPSc protease sensitivities and amyloid plaque content using RT-QuIC and eQuIC. *PLoS One* 7:e48969. <http://dx.doi.org/10.1371/journal.pone.0048969>.
 52. Orrú CD, Groveman BR, Hughson AG, Zanusso G, Coulthart MB, Caughey B. 2015. Rapid and sensitive RT-QuIC detection of human Creutzfeldt-Jakob disease using cerebrospinal fluid. *mBio* 6(1):e02451-14. <http://dx.doi.org/10.1128/mBio.02451-14>.
 53. Orrú CD, Wilham JM, Hughson AG, Raymond LD, McNally KL, Bossers A, Ligios C, Caughey B. 2009. Human variant Creutzfeldt-Jakob disease and sheep scrapie PrP(res) detection using seeded conversion of recombinant prion protein. *Protein Eng Des Sel* 22:515–521. <http://dx.doi.org/10.1093/protein/gzp031>.
 54. McGuire LI, Peden AH, Orrú CD, Wilham JM, Appleford NE, Mallinson G, Andrews M, Head MW, Caughey B, Will RG, Knight RSG, Green AJE. 2012. RT-QuIC analysis of cerebrospinal fluid in sporadic Creutzfeldt-Jakob disease. *Ann Neurol* 72:278–285. <http://dx.doi.org/10.1002/ana.23589>.
 55. Orrú CD, Hughson AG, Race B, Raymond GJ, Caughey B. 2012. Time course of prion seeding activity in cerebrospinal fluid of scrapie-infected hamsters after intratongue and intracerebral inoculations. *J Clin Microbiol* 50:1464–1466. <http://dx.doi.org/10.1128/JCM.06099-11>.
 56. Haley NJ, Van de Motter A, Carver S, Henderson D, Davenport K, Seelig DM, Mathiason C, Hoover E. 2013. Prion-seeding activity in cerebrospinal fluid of deer with chronic wasting disease. *PLoS One* 8:e81488. <http://dx.doi.org/10.1371/journal.pone.0081488>.
 57. Bessen RA, Wilham JM, Lowe D, Watschke CP, Shearin H, Martinka S, Caughey B, Wiley JA. 2011. Accelerated shedding of prions following damage to the olfactory epithelium. *J Virol* 86:1777–1788.
 58. Shi S, Mitteregger-Kretzschmar G, Giese A, Kretzschmar HA. 2013. Establishing quantitative real-time quaking-induced conversion (qRT-QuIC) for highly sensitive detection and quantification of PrPSc in prion-infected tissues. *Acta Neuropathol Commun* 1:44. <http://dx.doi.org/10.1186/2051-5960-1-44>.
 59. Henderson DM, Davenport KA, Haley NJ, Denkers ND, Mathiason CK, Hoover EA. 2015. Quantitative assessment of prion infectivity in tissues and body fluids by real-time quaking-induced conversion. *J Gen Virol* 96:210–219. <http://dx.doi.org/10.1099/vir.0.069906-0>.
 60. Chesebro B, Striebel J, Rangel A, Phillips K, Hughson A, Caughey B, Race B. 2015. Early generation of new PrPSc on blood vessels after brain microinjection of scrapie in mice. *mBio* 6(5):e01419-15. <http://dx.doi.org/10.1128/mBio.01419-15>.
 61. European Food Safety Authority. 2014. Protocol for further laboratory investigations into the distribution of infectivity of atypical BSE. *EFSA J* 12:3798.
 62. National Institute of Animal Health. 2001. Guide for the care and use of laboratory animals. National Agriculture and Food Research Organization, Tsukuba, Japan.
 63. Science Council of Japan. 2006. Guidelines for proper conduct of animal experiments. Science Council of Japan, Tsukuba, Japan. <http://www.scj.go.jp/ja/info/kohyo/pdf/kohyo-20-k16-2e.pdf>